Environmental Earth Sciences (2021) 80:659
https://doi.org/10.1007/s12665-021-09947-2

ORIGINAL ARTICLE

Evaluation of basin morphometric indices and tectonic implications in sedimentary landscape, Central India: A remote sensing and GIS approach

B. S. Manjare[1] · G. P. Obi Reddy[2] · Shradha Kamble[1]

Received: 23 July 2020 / Accepted: 5 September 2021 / Published online: 21 September 2021

Abstract

The present study was aimed to investigate the morphometric indices and tectonic implications in sedimentary landscape of Wardha River sub-basin, Central India. Geologically, the study area is predominantly constituted with Vindhyan and Lower Gondwana sedimentary formations. In the study, IRS-1D, LISS-III satellite data and Geographic Information System (GIS) techniques were used to compute morphotectonic indices *viz*., channel sinuosity (S), drainage basin asymmetry factor (AF), transverse topographic symmetry factor (T), basin elongation ratio (Re), drainage basin shape (Bs) and mountain front sinuosity (Smf) to determine the tectonic activity of the study area. The terrain parameters such as aspect, slope and relative relief, river longitudinal profile and topographic profile of the basin were also computed by using Shuttle Radar Topography Mission (SRTM) Digital Elevation Model (DEM) of 30 m spatial resolution. The computed S index for 69 meandering locations ranges from 1.03 to1.97, and it indicates the foremost courser of the river sinuous to meandering. The Re value ranges between 0.47 and 0.74, and it suggests the active to slight tectonic implications in the study area. The Smf values range from 1.14 to 4.69, and it indicates that the study area had slight to active tectonic implication. The T values range from 0.06 to 0.94, and it also indicates the tectonic activity. The present investigation clearly demonstrates the potential of remote sensing and GIS-based approach in evaluation of morphotectonic indices, which reveals the implications of tectonic activity in sedimentary landscape of Wardha River sub-basin, Central India.

Keywords Basin morphometry · Tectonics activity · Remote sensing · Geographic Information System · Sedimentary landscape · Central India

Introduction

Tectonic geomorphology is defined as the application of geomorphology to tectonic problems, and it includes the study of landform assemblage, landscape evolution, development of process response models of area and regions affected by recent tectonic activity (Keller 1986; Matošet al. 2016; Geurts et al. 2018; Buczek and Górnik 2020). Tectonic deformation causes change in channel slope, inducing variations in channel morphology, fluvial processes and hydrological characteristics of a river system (Roy and Sahu 2015). Drainage system is highly sensitive indicator of active tectonics (Jackson and Leeder 1993; Repasch et al. 2017). Basin morphometry is used as potential tool for the measurement and analysis of various geometrical properties of the terrain, which includes channel sinuosity (S), drainage basin asymmetry factor (AF), transverse topographic symmetry factor (T), basin elongation ratio (Re), drainage basin shape (Bs) and mountain front sinuosity (Smf). The advancement in remote sensing and Geographic Information System (GIS) reveals a new perspective and accurate analysis in drainage morphological studies, which also provides spatial information needed for integration of several geospatial databases in computation of morphometry indices (Mahala 2020). Systematic analysis of remotely sensed data helps in identification and delineation of landforms, structural features and evaluation of drainage characteristics more precisely (Reddy and Maji 2003; Reddy et al. 2004). The information derived

✉ B. S. Manjare
yogesh_manjare1@rediffmail.com

1 Department of Geology, RTM Nagpur University, Nagpur 444401, India

2 ICAR-National Bureau of Soil Survey and Land Use Planning, Amravati Road, Nagpur 440033, India

from digital elevation models (DEM) and topographical analysis of a basin in GIS is very effective and reliable in terms of their high accuracy (Prakash et al. 2016). The analytical capabilities of GIS are found very effective in performing hydrological modelling in conjunction with DEM, land use/land cover, soil texture and geology. (Liu and DeSmedt 2005; Youssef et al. 2016). DEM-based terrain visualization and quantification of topographic attributes made GIS a powerful tool in evaluation and analysis of various morphometric indices (Manjare 2013; Kumar et al. 2017; Reddy 2018). Computer visualization capabilities provide additional tools for geological mapping, which may improve the agreement of the determined geological units with the terrain parameters derived from DEM (Singh and Dowerah 2010; Suganthi and Srinivasan 2010). Many authors used DEM in conjunction with remote sensing in delineation of structural, drainage features and quantification of morphotectonic parameters in GIS environment (Reddy et al. 2002; Bhatt 2007; Manjare 2014; Reddy et al. 2004; Manjare 2015; Sharma and Sarma 2017; Pande et al. 2018). However, the literature on study of morphometric indices and tectonic implications in the study region is scanty. Basin morphometry provides an insight into the process driven changes such as drainage runoff, infiltration, basin evolution and tectonic framework.

Basin morphometry explains the morphological changes, which occurred during the long-term evolution process of drainage basins and its impact on landscape dynamics (Bali et al. 2012). Further, the effect of geomorphological processes shows their impact on tectonic activities, drainage systems and landscape development (Dehbozorgi et al. 2010; Argyriou et al. 2017). The computed geometrical parameters of the drainage basin afford substantial information about the surface topographic settings, subsurface lithological structures, erosion status, variations in slope and causes for diverse drainage patterns in a region. Numerous authors used basin scale morphometry as a tool to evaluate tectonic activity in different geological settings (Azor et al. 2002; Keller and Pinter 2002; Dehbozorgi et al. 2010; Motoš et al. 2016). Rivers in the foreland basin have responded and adjusted to slow and subtle active tectonic movements (Jain and Sinha 2005; Manjare 2017). The results of several morphometric indices can be combined in order to highlight tectonic activity and relative degree of tectonism in an area (Keller and Pinter 1996; Faghih et al. 2015). Altin (2012) studied various morphometric indices in the southern Bolkar mountain region, Turkey, and reported that anomaly in stream length gradient, steeped narrow valley, elongated basin and primary stage in a drainage network indicates a greater tectonic activity in the region. The topography of a region affected by recent and/or active tectonic process, such as faulting, can be an important factor in controlling geomorphic processes and determine the effect of faulting mechanism and the rate of tectonic activity on morphologic development of a region (Keller 1986; Raj et al. 2003). The sub-surface structural, tectonic and geological characteristics of the region determine the surface drainage and its morphometric properties (Perez-Pena et al. 2010). Many researchers tested the application of geomorphic indices in specific regions such as fault-generated mountain fronts or drainage basins and their sensitivity to active tectonics (Bull and McFadden 1977; Rockwell et al. 1984; Silva et al. 1992; Wells et al. 1988) as a valuable tool in tectonically different active regions for identifying geomorphic changes. The present-day tectonic activity can be evaluated by using geomorphic parameters, which have been widely used to recognise the indicators of landforms deformed or modified by active faults (Tepe and Sozbilir 2017). An integrated multi-disciplinary approach using geomorphological, structural and neo-tectonism found to be useful in evaluation of active tectonics (Wells et al. 1988). However, systematic efforts were not made in evaluation of basin morphometric indices and tectonic implications especially in Sedimentary landscape of Wardha River basin of Central India. Hence, the present study was aimed firstly to compute and analyse various morphometric indices and delineation of distinct geological and geomorphological units to understand the tectonic activities of the study area. Secondly, to analyse morphometric indices to understand the basin morphotectonic implications in Wardha River sub-basin of Central India.

Study area

The Wardha River sub-basin lies between 19° 39′ 00″ and 19° 52′ 30″ N latitudes and 79° 12′ 00″ and 79° 21′ 00″ E longitudes in Chandrapur district of Maharashtra, Central India and cover with an area of 34,652.0 ha. (Fig. 1). The study area was divided into three distinct watersheds (watershed I, II and III) based on the SRTM DEM by using 'hydrological tool' in GIS. Wardha River originates at an altitude of 777 m of above msl (mean sea level) in Satpura range near Khairwani village of Betul district of Madhya Pradesh, Central India. About 62.0% of the study area constitutes Vindhyan sedimentary formations represented by limestone, shale and shaly limestone. The remaining 23.0% of the study area represents Lower Gondwana sedimentary formations, which includes rocks of the Talchir, Barakar and Kamthi. Gondwana sedimentary formations are represented by sandstones, shale, carbonaceous shale and coal, which are characterized by black, compact, fine grained basalt with vesicular structures (Shradha 2019). The climate of the study area was characterised as hot summer and general dryness throughout the year except during the south-west monsoon season (June–September). The temperature rises

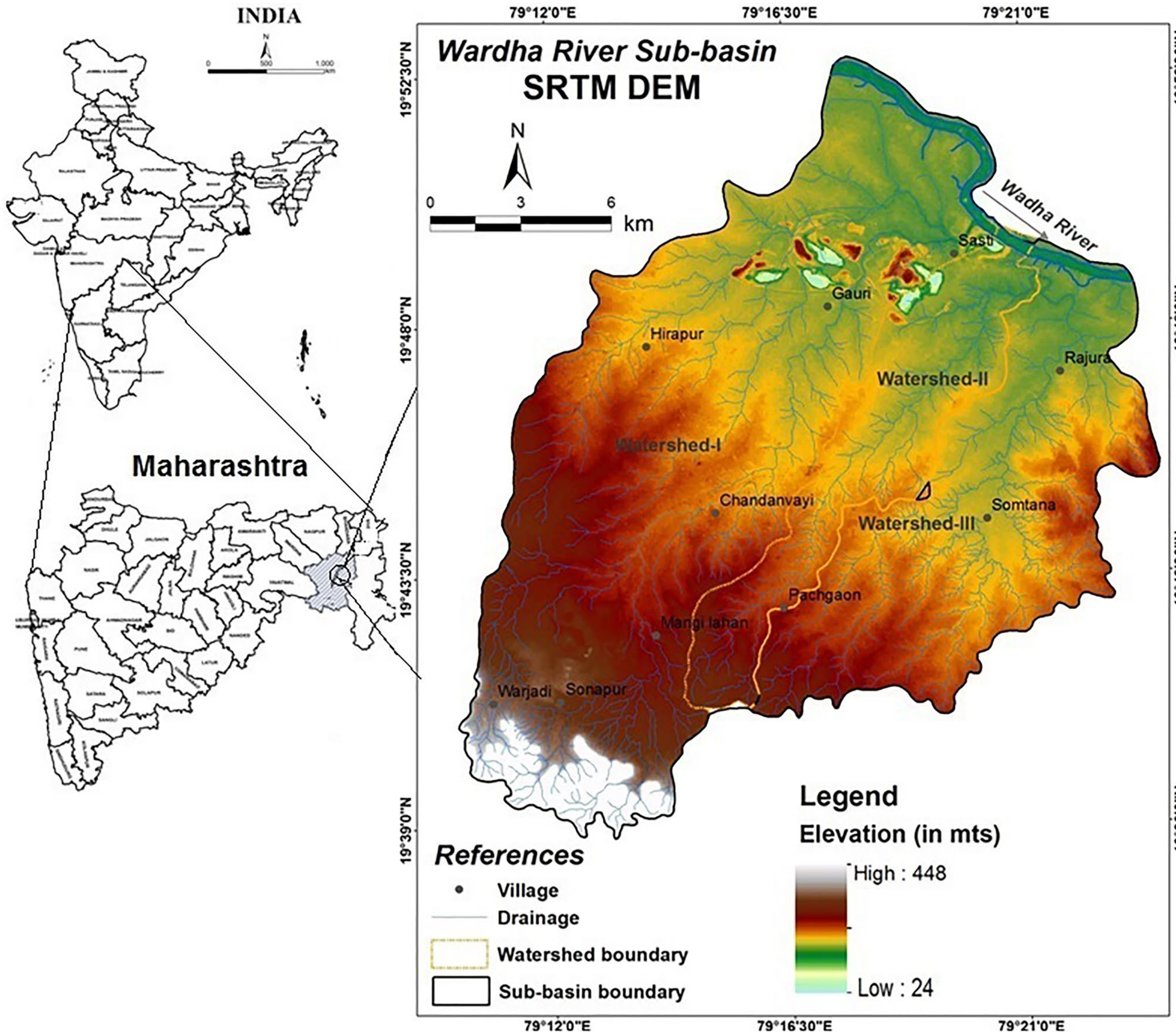

Fig. 1 Location map of the study area

rapidly after February till May, which is the hottest month of the year. The mean daily maximum temperature during May is 42.8 °C, and the mean daily minimum temperature during December is 12.2 °C. In the study area, dendritic to sub-dendritic drainage pattern is the most common pattern. However, at places, parallel to subparallel and rectangular drainage pattern was also observed (Shradha 2019).

Methodology

Datasets used

In the study, Survey of India (SOI) toposheets on 1:50,000 scale and District Resources Map (DRM) were obtained from Geological Survey of India (GSI 2002) and the same were used to delineate the distinct geological and geomorphological units. The obtained topographic maps were georeferenced and generated mosaic using ArcGIS. The IRS-1D, LISS-III satellite data of 6 November 2015 at 23.5 m spatial resolution were downloaded from Bhuvan Geoportal (https://bhuvan-app3.nrsc.gov.in/data/download/index.php) and georectified with the help of Survey of India (SOI) toposheets. IRS-1D, LISS-III data in conjunction with SOI toposheets were used to delineate distinct geomorphic units through visual interpretation by using onscreen digitation techniques in GIS. The Shuttle Radar Topography Mission (SRTM) v.4 DEM of 30 m resolution was downloaded from CGIAR–CSI (https://cgiarcsi.community/). The downloaded SRTM 30 m DEM was processed and analysed in ArcGIS (ver. 10.3) to compute various morphometric parameters of the study area. The drainage patterns of the study area were extracted using SRTM DEM (30 m) in Arc GIS. The satellite-based DEM's opened new avenues for geomorphologic studies including analysis of surface morphology (Reddy et al. 2018). The computation of morphotectonic parameter like channel sinuosity (S), drainage basin asymmetry (AF), transverse topographic symmetry (T), basin elongation ratio (Re), drainage basin shape (Bs) and mountain front sinuosity (Smf) were carried out by using the standard mathematical formulas. In the study, the terrain parameters such as aspect, slope and relative relief of the basin, river longitudinal profile and topographic profile were computed using SRTM DEM 30 m and rectified with necessary ground truth, wherever it was necessary. The topographic profiles and longitudinal river profiles were also carried out by using QGIS ver.3.2 software, and slope analysis was carried out by using ArcGIS software.

Terrain analysis using SRTM DEM (30 m)

Terrain analysis that includes, elevation, slope, aspect, topographic profiles and longitudinal profiles of the study area was carried out by using SRTM DEM 30 m. DEM analysis is extremely useful for analysing the elevation-related attributes of a fault zone area (Duncan et al. 2003). The tonal variations as depicts through elevation differences assisted in analysis of regional topography and structural features (Duncan et al. 2003; Hooper et al. 2003; Ganas et al. 2005). Topographic cross profiles aligning NW–SE were obtained from the DEM to visualize elevation characteristics in the upland and the alluvial zone. Longitudinal profiles of the trunk streams found in the three watersheds were also obtained. River longitudinal profiles are one of the indicators of active tectonics as they reflect the balance between erosion and uplift (Schumm et al. 2000; Keller and Pinter 2002; Molin and Fubelli 2005; Menéndez et al. 2008; Bull 2009). The topographical characteristics of a basin were determined by using the relative relief of catchment area (Gayen et al. 2013).

Delineation of distinct geological and geomorphological units

The geological and geomorphological units of the study were mapped by analysing the geo-coded IRS-ID, LISS-III data and district resources map (DRM) with necessary field verifications. The sedimentary landscape has been investigated to examine the implications of Quaternary neotectonic activities on drainage system through study of fluvial geomorphology, morphotectonics and digital terrain analysis using topographic maps on 1:50,000 scale, SRTM DEM (30 m), multi-spectral IRS LISS-III data of 23.5 m resolution and field surveys. In the study, visual interpretation techniques have been followed in delineation of distinct geological and geomorphological units based on the image characteristics like tone, texture, shape, drainage pattern, colour, associations and differential erosion characteristics of the satellite imagery along with field parameters such as topography, relief, surface cover, soil and vegetation cover. Additionally, extensive field observations have been carried out, which helped in confirming, consolidating and interpreting the results obtained from the geomorphic analysis. The lithological analysis of the study area was carried out through visual interpretation of the satellite data in conjunction with district resources map of Geological Survey of India (GSI 2002). Subsequently, detailed geomorphic units were delineated with the help of relief, morphometry and image characteristics. Based on the interpretation of satellite data in conjunction with SOI toposheets, district recourse map and field surveys, the distinct geomorphical units of the study area were delineated. Geomorphologically, the area was broadly classified into dissected plateau, pediments and plains based on the major geomorphic processes and agents involved in their transformation. These units are distinct with respect to their lithology, structure and evolution. Further, these units were sub-divided into structural hills, denudational hills, residual hills, plateau top, upper, middle, lower plateau, younger and older flood plain.

Computation of morphotectonic indices

Morphometric properties of drainage basins were widely used as good indicators to study the structural influence on drainage development and neotectonic activity (Das et al. 2011; Demoulin 2011). In the present study, the geometric parameters, which includes relative parameter, length area relation, form factor, shape factor ratio, elongation ratio, circulatory ratio, and compactness coefficient were computed for three watersheds by using GIS techniques. The morphometric properties of surface drainage were determined by the sub-surface structural, tectonic and geological characteristics of the region. The analysis of various morphometric parameters enables to evaluate the relationship between tectonic geomorphology and the landscape dynamic process (Reddy et al. 2004). In the study, various morphometric indices like channel sinuosity (S), drainage basin asymmetry factor (AF), transverse topographic symmetry factor (T), basin elongation ratio (Re), drainage basin shape (Bs) and mountain front sinuosity (Smf) were computed to analyse the degree of tectonic activity and its implications on drainage morphometry in the area. The following morphotectonic indices were computed by using the mathematical expressions given in Table 1.

Table 1 Computed morphotectonic indices and formulae used in the study area

Morphotectonic indices	Formulae	Inferences	Range in study area	References
Channel sinuosity (S)	S = SL/VL, where, SL = Stream length, VL = Valley length	S = 1.0, Straight Course S = 1.0–1.5, Sinuous Course, S > 1.5, Meandering Course	1.03–1.97	Muller (1968)
Drainage basin asymmetry factor (AF)	AF = 100(Ar/At), where, Ar = Right hand side area of drainage looking downstream & At = Total area of drainage basin	AF = 50, Stable setting environment AF > 50, Suggest tilt	23.61–49.20	Cox (1994)
Transverse topographic symmetry factor (T)	T = Da/Dd, Where, Da = Distance from middle of drainage basin of active channel, Dd = Distance from basin midline to basin divide	T = 0, Symmetric basin T > 0, Asymmetry basin	0.06–0.94	Cox (1994)
Basin elongation ratio (Re)	$Re = (2\sqrt{A}/\sqrt{\Pi})/L$, Where, A = Basin area, L = Basin length $\sqrt{}$	Re < 0.50, Tectonically active, Re = 0.50—0.75, Slightly active, Re > 0.75, Inactive settings	0.47–0.74	Bull and McFadden (1977)
Drainage basin shape (Bs)	$B_s = B_l / B_w$ (Define the planimetric shape of a basin) Where B_w = the width of the basin, B_l = the length of the basin	High Bs values = elongated basins, i.e. high tectonic activity; low Bs values = circular basins, i.e. low tectonic activity	1.70–3.79	(Bull and McFadden 1977); Cannon (1976)
Mountain front sinuosity (Smf)	Smf = Lmf/Ls, Where Lmf = Mountain front length along mountain foot, Ls = Straight line length of mountain front	Smf < 1.4, Tectonically active, Smf = 1.4–3, Slightly active, Smf > 3, Inactive setting	1.14–4.69	Bull and McFadden (1977)

Results and discussion

Terrain characterization

The aspect of watersheds derived from SRTM 30 m clearly indicates north, northwest, south and southwest facing slope of the basin. These major slopes reflect the higher moisture content and low evaporation that the other parts of the basin, which plays an important role to conserve vegetation, forests, and bio-diversity in the study area. The slope elements depend on rock type of its catchment with varying resistance and are highly related to run-off of the water, which affects the required time for rain water to enter in the river beds that make up the network of the river basin (Magesh et al. 2014). The slope of watersheds varies from level to nearly level (0–1%) to steeply sloping (> 30%) (Fig. 2). In general, the longitudinal river profiles show steeper slopes in the uplands reach and lower slopes in the alluvial reach. Majority of the streams exhibit knick-points in the resistant rocks of the uplands and concave-up shapes with straight reaches in the less-or non-resistant alluvial lithology (Fig. 3a). The knickpoints are located close to the intersection of lithological contacts and fracture zones. The longitudinal river profiles of watershed

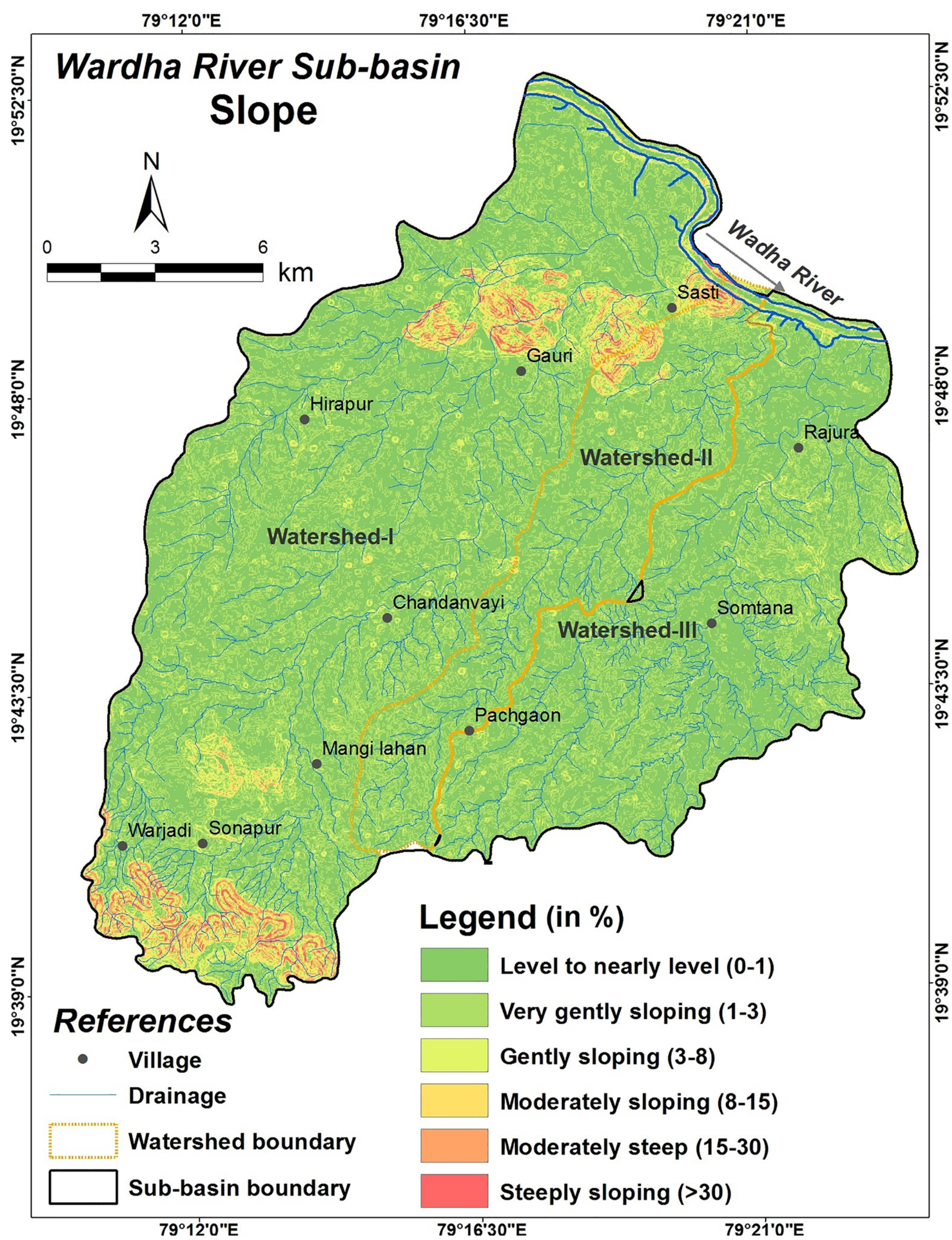

Fig. 2 Slope map of the study area

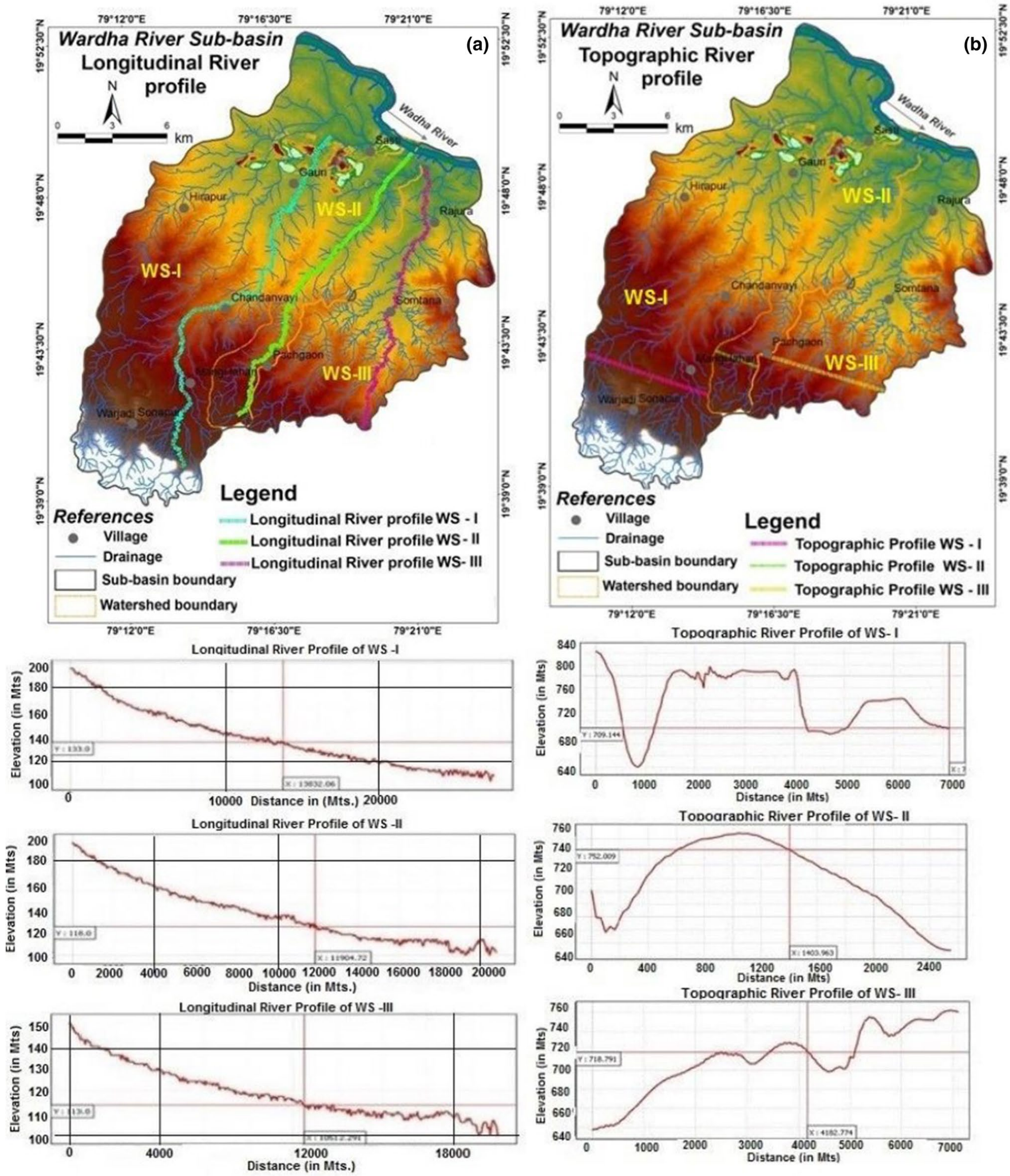

Fig. 3 **a** Longitudinal river profiles and **b** Topographic river profiles of three watersheds drawn on SRTM DEM

I, II and III shows steep gradients in the upland reaches, which contrasts with the graded, but steeper profiles in other part of the reach. The longitudinal river profile shows good correspondence with the weaker incision in segment, and distinct convex-up morphology in study area. The topographical characteristic of a basin is determined by using the relative relief of its catchment area (Gayen et al. 2013). The study area have highest relief of 448 m, while the lowest value was measured as 24 m. The low relief designated in the southwest side suggests that this area of the basin is flat to gentle slope type (Fig. 3b). In the study area, three topographic profiles *viz.*, Topographic profile I A-A', Topographic profile II D-D' and Topographic profile III G-G' were studied and noticed high degree of topographic variations at higher elevation. The topographic profile I A-A' suggested that most variations in the topography of convex-up shape in the topography of the area while in topographic profile II D-D' shows the slope at both sides, it clearly shows the northward and southward tilt of the non-resistant rocks of the profile and topographic profile III G-G' shows the undulating topography.

Geological and geomorphological setting

Geologically, the study area is mainly characterised by Vindhyan and Lower Gondwana sedimentary formations and Quaternary alluvium. Wardha River sub-basin constituted of Vindhyan sedimentary formations represented by limestone, shale and shaley limestone, Lower Gondwana sedimentary formations characterized by Talchir, Barakar and Kamthi, whereas Gondwana sedimentary formations are represented by sandstones, shale, carbonaceous shale and coal (Fig. 4a). Wardha River and its major streams have developed the flood plains along their banks. It comprises sand, silt and clay. Black cotton soil and sandy soil deposits were found at the average height of 5–10 m above the stream level. In case of Wardha River, at places these deposits were found with 100–300 m wide and up to the height of 15 m along the course of major stream (GSI 2002 and Table 2).

Geomorphologically, the dissected plateau covers in eastern part of the study area and it can be characterised as plateau area that has been severally eroded as a result the relief becomes sharp and it can be distinguishable from orogenic mountain belts by the lack of folding, metamorphism, extensive faulting, or magmatic activity. This geomorphic unit is predominantly covered by open forest known as Rajura reserved forest near to Rajura villages and southern part area near Sonapur and Warjadi. Pediments are a very gently sloping inclined bedrock surface and found in the eastern part of the study area near to Rajura, Somtana and Kothaguda villages. Pediments are typically slope down from the base of steeper escarpment,

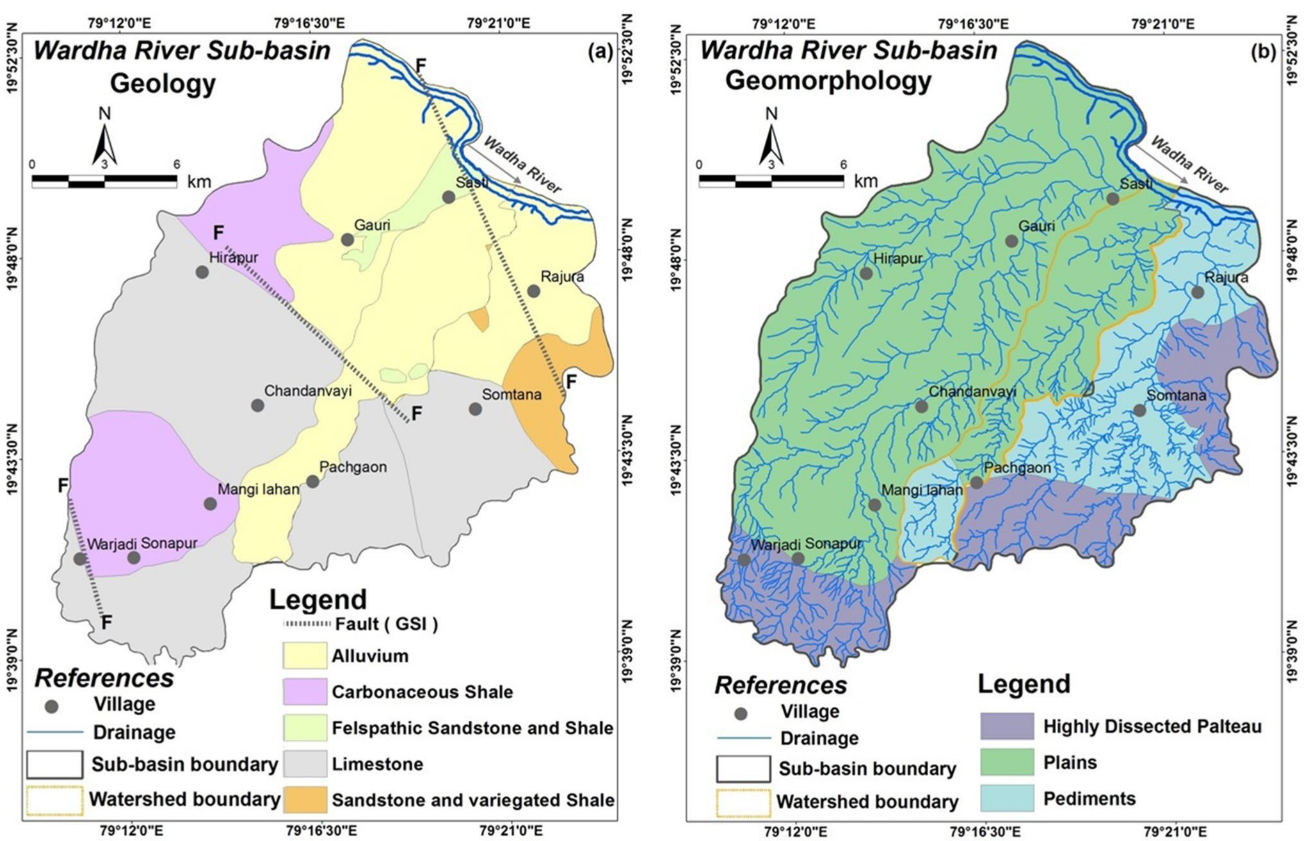

Fig.4 **a** Geological units and **b** Geomorphological units of the study area

Table 2 Stratigraphy of the study area

Age	Group / formation	Lithology
Quaternary	–	Alluvial gravel beds, black cotton soil Basalts -----Unconformity-----
Cretaceous	Lameta formation	Limestones, Cherts and Silicified sandstones -----Unconformity-----
Upper Triassic	Maleri Formation	Fine to medium grained sandstone and red shale Red, brown and variegated sandstones, reddish siltstones and variegated shales
Upper Permian to Lower Triassic	Kamthi formation	-----Unconformity----- Light grey to white sandstones, shales and coal seams Tillites, turbidites, varves, needle shales and sandstones
Lower Permian	Barakar formation	-----Unconformity-----
Upper Carboniferous to Lower Permian	Talchir formation	White to brown quartzitic sandstones, conglomer blue pink Limestones and Chertsate Quartzites, granite gneisses, etc -----Unconformity-----
Precambrian	Sullavai Group	
Archaean	Pakhal Group	

Source: GSI (2002)

but may continue to exist after the mountain eroded away. It develops when sheets of running water wash over it during the intense rainfall events. Plains are the area between piedmont zone and the main river, which are relatively level area and exhibits gentle slopes and small local relief. The area of plains ranges from few hectares to hundreds of thousands of square kilometers. The plains of the study area are basically represented by the presence of pediplains and flood plain of Wardha River. In study area, the flood plains are noticed around Sasti, Gauri, Hirapur, Chndanvayi, Dhoptala, Khamona and Panderponi villages (Fig. 4b).

Morphometric indices

Channel sinuosity (S)

Channel sinuosity (S) is used to understand the role of tectonism on landform formation (Muller 1968; Susan 1993). The sub-surface geological structures can influence the geometric structure of the drainage network of an area, which can be identified by channel sinuosity indices (Litchfield et al. 2003). In general, no river follows a straight course from source to the mouth. Many causative factors such as geographical, topographical and hydrological influence it to deviate from its straight course. The channel sinuosity analysis helps in understanding the effect of terrain characteristics on the river course and vice versa. The channel sinuosity index value of one indicates straight river course and values between 1.0 and 1.5 indicate sinuous river shape, whereas, channel sinuosity (S) values more than 1.5 represent meandering course. Sinuosity parameters for study area were computed at sixty-nine channel segments numbered from 1 to 69. Out of sixty-nine segments, nine channel segments have value smaller than 1.0, which exhibits the straight course and forty-four channel segments have value between 1.0 and 1.5, which exhibits sinuous course and sixteen channel segments have value greater than 1.5 shows meandering course (Fig. 5a and Table 3).

Drainage basin asymmetry factor (AF)

The AF is typically applied to identify the tectonic control over basin evolution at the regional and local scales (Cox 1994; Hare and Gardner 1985). AF index is also used to evaluate the active tectonic tilting within the drainage basin and to determine the direction of tilting (Kale et al. 2014; Siddiqui 2014). Drainage basins with AF value significantly greater or smaller than 50 are known as asymmetric basins. AF values are close to 50 in symmetric basins that have developed under stable conditions with little or no tilting (Hare and Gardner 1985; Keller and Pinter 2002). If AF values are greater than 50, the channel has changed direction towards the downstream left; if values are less than 50, the channel has shifted towards the downstream right (Scotti et al.2014). In the present study, AF value of watersheds (WS-I, WS-II, WS-III) with calculation of basin right trunk and left trunk area ranges from 50.96 to 73.44, which infers that the suggested basin is tilted towards left as the asymmetry factor value is not equal to 50 (Fig. 5b and Table 4).

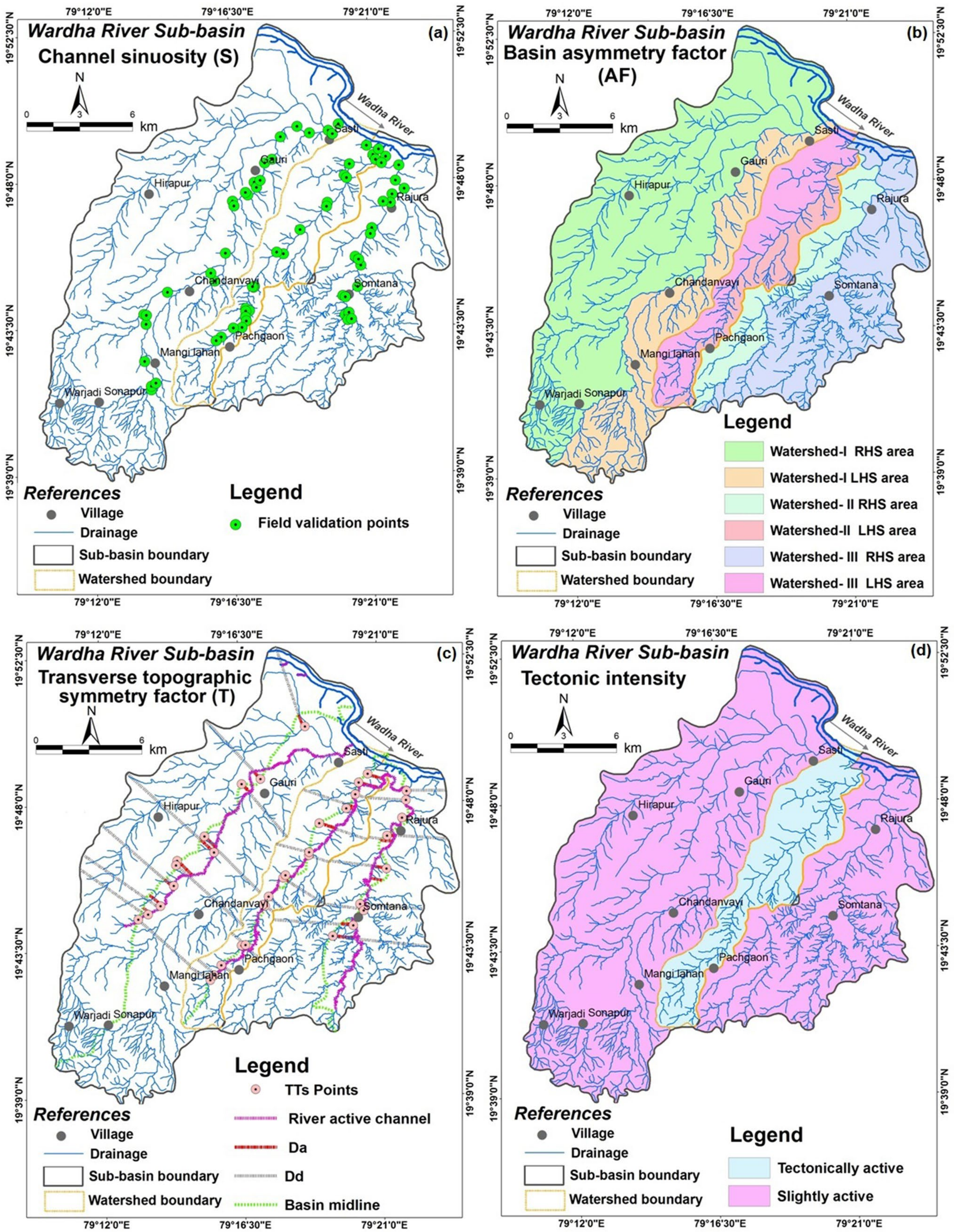

Fig. 5 **a** Channel sinuosity (S), **b**: Drainage basin asymmetry factor (AF); **c** Transverse topographic symmetry factor (T) and **d** Tectonic intensity of three watersheds in the study area

Table 3 Computed channel sinuosity segments of three watersheds of the study area

S. No	Watershed code	Stream Length (SL) m	Valley length (VL)m	Channel Sinuosity (S)	Inferences
1	WS -1	414.88	393.89	1.05	Straight course
2	WS -1	462.49	326.41	1.41	Sinuous course
3	WS -1	262.46	233.03	1.12	-do-
4	WS -1	142.78	126.48	1.12	-do-
5	WS -1	505.64	457.37	1.10	-do-
6	WS -1	193.95	173.65	1.11	-do-
7	WS -1	287.00	258.63	1.10	-do-
8	WS -1	550.49	489.63	1.12	-do-
9	WS -1	358.81	332.18	1.08	Straight course
10	WS -1	544.63	335.49	1.62	Meandering Course
11	WS -1	143.70	127.90	1.12	Sinuous course
12	WS -1	177.82	167.96	1.05	-do-
13	WS -1	228.69	160.68	1.40	-do-
14	WS -1	286.77	237.92	1.20	-do-
15	WS -1	299.10	273.00	1.09	-do-
16	WS -1	597.64	418.95	1.42	-do-
17	WS -1	716.43	299.91	2.38	Meandering course
18	WS -1	713.21	487.58	1.46	Sinuous course
19	WS -1	242.76	219.22	1.10	-do-
20	WS -1	127.23	95.24	1.33	-do-
21	WS -1	270.17	220.57	1.22	-do-
22	WS -1	155.94	124.55	1.25	-do-
23	WS -1	275.07	198.79	1.38	-do-
24	WS -1	242.04	182.86	1.32	-do-
25	WS -1	184.97	143.16	1.29	-do-
26	WS -1	284.19	165.29	1.71	Meandering course
27	WS-2	644.49	344.56	1.87	Meandering course
28	WS-2	411.94	344.56	1.23	Sinuous course
29	WS-2	459.83	347.16	1.32	-do-
30	WS-2	369.54	288.92	1.27	-do-
31	WS-2	216.64	181.60	0.83	-do-
32	WS-2	234.82	191.79	1.22	-do-
33	WS-2	189.89	165.69	1.14	-do-
34	WS-2	264.60	214.13	1.07	-do-
35	WS-2	251.15	231.18	1.08	-do-
36	WS-2	386.93	295.37	1.30	-do-
37	WS-2	301.22	268.29	1.12	-do-
38	WS-2	122.41	101.70	1.20	-do-
39	WS-2	103.75	84.21	1.23	-do-
40	WS-2	87.53	137.55	1.14	-do-
41	WS-2	327.30	260.83	1.81	Meandering course
42	WS-2	366.87	97.92	3.74	Meandering course
43	WS-2	187.69	133.89	1.04	Straight course
44	WS-2	164.82	102.25	1.61	Meandering course
45	WS-2	216.64	147.08	1.47	Sinuous course
46	WS-2	419.64	287.18	1.46	-do-
47	WS-2	142.75	126.73	1.12	-do-
48	WS-2	244.92	226.51	0.99	-do-
49	WS-2	155.88	136.04	1.14	-do-
50	WS-3	581.61	432.72	1.34	-do-

Table 3 (continued)

S. No	Watershed code	Stream Length (SL) m	Valley length (VL)m	Channel Sinuosity (S)	Inferences
51	WS-3	463.59	342.02	1.35	-do-
52	WS-3	911.89	514.20	1.77	Meandering course
53	WS-3	938.29	756.52	1.24	Sinuous course
54	WS-3	663.29	421.24	1.57	Meandering course
55	WS-3	512.97	364.83	1.40	Sinuous course
56	WS-3	637.24	366.24	1.73	Meandering course
57	WS-3	1013.80	534.19	1.89	-do-
58	WS-3	425.66	384.96	1.10	Sinuous course
59	WS-3	285.48	263.47	1.08	-do-
60	WS-3	382.23	183.23	2.07	Meandering course
61	WS-3	381.19	194.96	1.95	Meandering course
62	WS-3	356.08	292.00	1.21	Sinuous course
63	WS-3	514.79	346.68	1.48	-do-
64	WS-3	328.86	116.78	2.04	Meandering course
65	WS-3	223.80	183.76	1.22	Sinuous course
66	WS-3	251.80	108.77	2.31	Meandering course
67	WS-3	288.90	79.72	3.62	-do-
68	WS-3	450.71	260.49	1.73	-do-
69	WS-3	182.27	132.47	1.37	Sinuous course

Table 4 Drainage basin asymmetry factor (AF), RHT-right hand trunk and LHT-left hand trunk in the study area

S. No	Watershed code	RHT area in Sq.Km (Ar)	LHT area Sq.Km	Total area of watershed (At)	Asymmetric factor (Af)	Inferences
1	WS-I	147.44	53.32	200.76	73.44	Suggest Tilt
2	WS-II	28.24	21.5	49.74	56.77	-do-
3	WS-III	48.94	47.08	96.02	50.96	-do-

Transverse topographic symmetry factor (T)

The T values of the watersheds indicate the migration of streams perpendicular to the drainage basin axis. The T is a vector that ranges from zero to one ($T = 0– < 1$), which reflects a perfect asymmetric basin or a tilted one, respectively (Burbank and Anderson 2000; Cox 1994; Cox et al. 2001; Keller and Pinter 2002). In case of a negligible influence by the bedrock tilting on the relocation of the stream channels, the direction of the regional migration is an indicator of the ground tilting in that similar direction. The analysis of numerous drainage basins in an area results in multiple spatially distributed T vectors, which, when averaged, define the irregular zones of basin asymmetry. The calculation of both AF and T factors is a quantitatively rapid method of identifying ground tilting (Cox 1994; Cox et al. 2001; Keller and Pinter 2002). The completely symmetric basin has T value of zero, whereas, the asymmetry basin increases T and approaches to value of 1.0. In the study area, the computed T values of 3 watersheds ranges from 0.01 to 0.82 and indicates the asymmetric nature of the study area as the T values are greater than zero (Fig. 5c and Table 5). The higher T values of an areas indicate the potential tilting influence on drainage pattern. It was evidenced from the study that these watersheds have sudden change in drainage pattern, it leads to deposition of alluvium and changes in lithology near Rajura village.

Table 5 Transverse topographic symmetry factor (T) values of three watersheds of the study area

S. No	Watershed code	(Da)	(Dd)	T = Da/Dd	Topographic Symmetry(T)
1		853	4029	0.21	Asymmetric basin
2	WS-1	658	4582	0.14	-do-
3	WS-1	1032	5622	0.18	-do-
4	WS-1	727	4756	0.15	-do-
5	WS-1	953	4398	0.21	-do-
6	WS-1	894	3461	0.25	-do-
7	WS-1	99	3386	0.02	-do-
8	WS-1	956	1272	0.75	-do-
9	WS-1	923	4490	0.20	-do-
10	WS-1	718	4018	0.17	-do-
11	WS-2	1070	1514	0.70	Asymmetric basin
12	WS-2	110	701	0.15	-do-
13	WS-2	506	1455	0.34	-do-
14	WS-2	1006	2872	0.35	-do-
15	WS-2	32	1244	0.02	-do-
16	WS-2	325	2401	0.13	-do-
17	WS-2	118	995	0.18	-do-
18	WS-2	139	524	0.26	-do-
19	WS-2	376	1210	0.31	-do-
20	WS-2	207	623	0.33	-do-
21	WS-2	636	1793	0.35	-do-
22	WS-2	82	1444	0.05	-do-
23	WS-2	447	1071	0.41	-do-
24	WS-2	38	1925	0.01	-do-
25	WS-2	354	2757	0.12	-do-
26	WS-3	190	2293	0.08	Asymmetric basin
27	WS-3	361	1233	0.29	-do-
28	WS-3	549	3422	0.16	-do-
29	WS-3	631	4365	0.14	-do-
30	WS-3	257	3629	0.07	-do-
31	WS-3	1489	5659	0.26	-do-
32	WS-3	595	3987	0.14	-do-
33	WS-3	442	2446	0.18	-do-
34	WS-3	800	3244	0.24	-do-
35	WS-3	638	778	0.82	-do-
36	WS-3	122	2307	0.05	-do-

Table 6 Basin elongation ratio (Re) of the three watersheds of the study area

S.No	Watersheds	Area (sq/km)	Length (m)	Elongation ratio (Re)	Inference
1	WS-I	200.76	25,244.69	0.63	Slightly active
2	WS-II	49.74	18,188.43	0.43	Tectonically active
3	WS-III	96.02	17,244.86	0.56	Slightly active

Table 7 Computed drainage basin shape (Bs) of three watersheds in the study area

S.No	Watersheds	Bl (km)	Bw (km)	Bs	Inference
1	WS-I	24,977.68	9097.81	2.92	Elongated basin
2	WS-II	18,397.54	4338.90	4.24	-do-
3	WS-III	17,262.51	7266.79	2.37	-do-

Basin elongation ratio (Re)

The Re is the ratio of the diameter of a circle representing the same area of the basin to its length. The value of Re approaches 1 if the basin shape is almost like a circle. As proposed by Bull and McFadden (1977), the Re is one of the proxy indicators of neotectonics activity (Cuong and Zuchiewicz 2001). Drainage basins in arid and semi-arid climates show Re value less than 0.50 and between 0.50 and 0.75 for tectonically active settings (Bull and McFadden 1977). The basin elongation ratio (Re) values are calculated for three watersheds in the study area, and elongation ratio (Re) values range between 0.43 and 0.63. The Re value of WS-I and WS-III indicates that these watersheds are slightly active as they range from 0.63 to 0.56, while on the other hand watershed WS-II is less than 0.50, which infers the tectonically active region (Table 6). In the study area of Sasti and Chandanvayi, watersheds show the tectonically activeness. The Re and its relevance to tectonic activeness in the watersheds (WS-I, WS-III) were analysed, and it inferred that the WS-II is most prone to tectonic activity (Fig. 5d and Table 6).

Drainage basin shape (Bs)

The Bs describes the planimetric shape of a basin (Canon 1976; Ramírez-Herrera 1998). Basins with elongated shapes characterize active mountain range areas while after cessation of mountain uplift their shapes became more circular (Bull and McFadden 1977). The index depicts difference between elongated basins with high values of Bs, and more circular basins with low values. The high values of the basin indicate its tectonic deformation (Burbank and Anderson 2001; Ramírez-Herrera 1998). In the study area, basin shape values of three watersheds range from 2.37 to 4.24 (Table 7). The value of Bs shows that the watersheds in the sub-basin are elongated and indicate their tectonic activity.

Mountain front sinuosity (Smf)

*S*mf is an index that reflects the balance between erosional processes that tend to yield irregular and sinuous fronts and tectonic forces that tend to maintain a comparatively straight front (Bull 1977; Bull and McFadden 1977; Keller 1986; Keller and Pinter 2002; El-Hamdouni et al. 2008). In tectonically active mountain, fronts tend to have low values of *S*mf, as they have not experienced significant range front erosion and responding to active tectonic uplift on a relatively steep fault, keeping the front straight. At less active fronts, where erosional processes overcome tectonic processes, irregular or sinuous fronts with higher values of *S*mf occur. In some of the recent studies, the *S*mf values indicate down to 1.4, and it is an indicative of a tectonically active front (Bull 1977, 1978; Bull and McFadden 1977; Wells et al. 1988; Burbank and Anderson 2000; Keller and Pinter 2002). If the value of *S*mf is higher than 3, it indicates an inactive front in which the initial range–piedmont fault might be more than 1 km from the present erosional front (Bull 1977, 1978; Bull and McFadden 1977; Burbank and Anderson 2000; Keller and Pinter 2002).

Mountain fronts and tectonic implications

Both Lmf and Ls are measured physically in the same units as the topographic map scale then fed into the equation to obtain results; thus, the Smf index is unit less (Bull 1977, 1978; Bull and McFadden 1977; Keller and Pinter 2002; Rockwell et al. 1984; Wells et al. 1988). Mountain fronts can be calculated as one front divided into segments of approximately 1 km long or as several continuous fronts of various lengths (Bull

Table 8 Computed mountain front sinuosity (Smf) along the two fronts in the study area

S.No	Lmf(m)	Ls(m)	Smf(m) = Lmf/Ls	Inference
1	956	620	1.5	Slightly active setting
2	1539	761	2.0	-do-
3	1106	901	1.2	Tectonically active setting
4	2317	773	2.9	Slightly active setting
5	630	582	1.0	Tectonically active setting
6	1589	583	2.7	Slightly active
7	714	141	5.0	Inactive setting
8	2370	357	6.6	-do-
9	764	432	1.7	Slightly active setting

1978; Wells et al. 1988). The latter approach has been adopted in this study since it is widely used and is more suitable to the present study area. Intersection with cross-cutting drainages large in scale relative to the front, abrupt deflections in mountain front orientation, abrupt changes in lithology and changes in the main geomorphic characteristics of a mountain front relative to adjacent front segments such as relief, steepness, or dissection (Wells et al. 1988). In the study area, Smf values were computed from the front 1 and front 2. The Lmf and Ls values were calculated front 1 to front 9 (Table 8). The first mountain front (Front 1, segments 1–5) is about 6.97 km and taken near Warjadi and Sonapur villages. Segments first and second have slightly active setting, segments third and fifth shows tectonically active setting, while segment fourth shows slightly active settings (Table 8). The second front (front 2, segments 6–9) is 12.26 km, which was taken for analysis near Rajura, Kapangoan and Somtana village. Segment number six is slightly active, while segments seven and eight are inactive in nature, and segment nine is slightly active (Table 8).

Filed evidences of tectonic activity

The rock strata in the study area are mainly characterised by Vindhyan sedimentary formations of Talchir and Barakar and Lower Gondwana sedimentary formations of Kamthi and Quaternary alluvium as observed in the field along the Wardha River. The Sandstones in the region are fractured and jointed near Sasti and Rajura village (Fig. 6a, b). During the field survey, many significant meandering patterns were observed along the Wardha River (Fig. 6c, d.) There meandering patterns might be developed due to the tectonic upliftment, and it indicates the active tectonics in the study area. River terraces formed by lateral erosion of main stream as an eroded floodplain generally separated from the new floodplain by a steep-slope. This might have formed when vertical erosion occurs in a floodplain that was previously being formed by the normal condition of deposition and lateral erosion. The height and internal composition of river terraces contributes significantly to understand the geological history of the river course and the climatic evolution of the region as they affected by the rainfall, flood patterns and the geomorphological process of river terraces. In study area, well developed river terraces were observed along the Wardha River near the Sasti village and Rajura village (Fig. 6e, f). Triangular facets can be significantly seen on satellite image, which are generally formed by the erosion of fault bounded small mountain ranges. Triangular facets are most prominent geomorphic features frequently observed on active normal fault scarps and fault line scarp and also observed in regions of active extension such as the sub-basin and range (Cotton 1950; Wallace 1978). Balogun et al. 2011 suggested that triangular facet development has facet size and slope exhibit a strong linear dependency on fault slip rate. Triangular facets in the study area have been observed near Sonapur village. These might have developed due to the tectonic activity in the study area (Fig. 6g, h).

Conclusions

The study clearly demonstrates the potential of morphometric indices derived from remote sensing, GIS and field studies, which gave ample inferences of tectonic evidences in the study area. The sixty-nine segments were studied for the tectonic study and out of which, forty-four channel shows sinuous course, and sixteen segments show meandering course, and remaining segments show straight course, which is less than 1.0. The WS-I, WS-II and WS-III shows AF value as 73.44, 56.77, and 50.96, respectively, which clearly inferred that the basin has tilt. The analysis of T values of thirty-six segments of three watersheds shows that the value ranges from 0.01 to 0.82, which clearly suggested that the watersheds are asymmetric in nature. The Re values of WS-I and WS-III shows the value of 0.63 and 0.56, respectively, which inferred slightly active setting, and WS-II gives the value 0.43, which is less than 0.50 and show tectonically active setting. The Smf values of two fronts shows that the value of two segment has 5.0 and 6.6, which is greater than 3; hence, they show inactive setting and the five segment shows the Smf value between 1.4 and 3 and show slightly active in nature. The remaining segments show the Smf value of smaller than 1.4, which suggests that they are tectonically active in nature. The Bs value of three watersheds found to be high, and it indicates elongated basin and tectonically active in nature. The longitudinal and topographic river profiles shows linear to exponential model, which implies less concavity in their profiles; thus, it evidences of disturbances in the course of the rivers and implications of recent tectonic movements as evidenced through morphotectonic parameters.

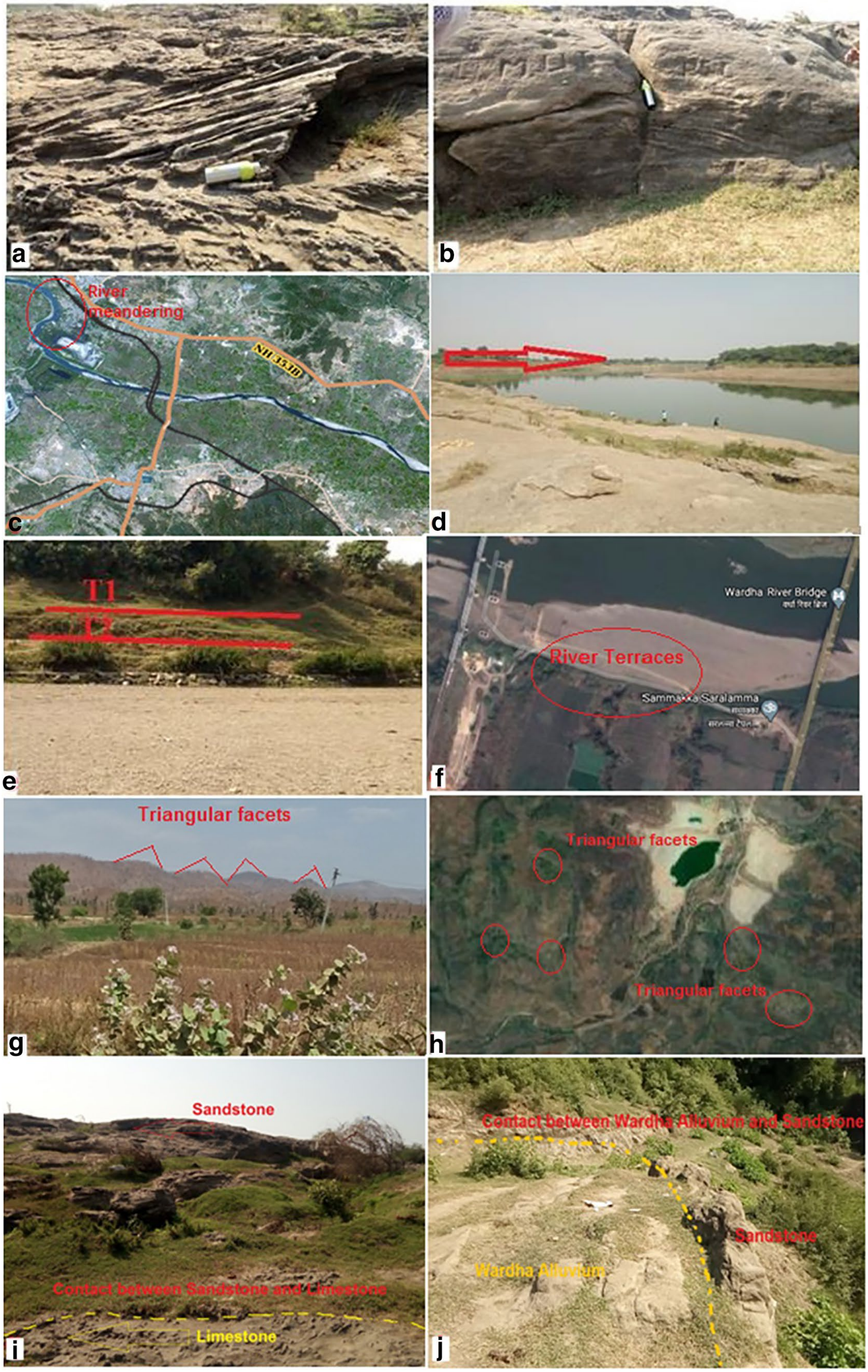
a
b
River meandering
NH 353B
c
d
T1
T2
e
Wardha River Bridge
River Terraces
Sammakka Saralamma
f
Triangular facets
g
Triangular facets
Triangular facets
h
Sandstone
Contact between Sandstone and Limestone
Limestone
i
Contact between Wardha Alluvium and Sandstone
Sandstone
Wardha Alluvium
j

Fig. 6 Filed evidences of tectonic activity **a** Fractured Kamthi Sandstone and **b** jointed Kamthi Sandstone along Wardha River near Sasti and Rajura village **c** meandering of Wardha as shown on Google image **d** observation of meandering of Wardha River near Sasti village **e** observation of river terraces along Wardha River near Rajura village **f** river terraces observed on Google image **g** observation of triangular facets near Sonapur village **h** of triangular facets on Google image and **i** and **j** Evidences of alluvium deposition and sudden change in lithology near Rajura village, respectively

Acknowledgements The first author of the paper thanks to University Grants Commission (UGC) of India SAP DRS Phase II for financial support to carry out the research work (Letter. No.F.550/2/DRSII/2016, SAP-II). The author also thanks to Head of Department, Department of Geology, RTM, Nagpur University, Nagpur for all necessary support to carry out the work. Authors also thanks to ISRO-Bhuvan geoportal (https://bhuvan-app3.nrsc.gov.in/data/download/index.php) and CGIAR–CSI (https://cgiarcsi.community/) for sharing the IRS-ID, LISS-III data SRTM v.4 DEM of 30 m resolution DEM for the study area, respectively. We also sincerely thank the reviewers for their constructive comments/suggestions, which helped greatly to improve the overall quality of manuscript.

References

Altin TB (2012) Geomorphic signatures of active tectonic in drainage basins in the southern Bolkar mountain Turkey. J Indian Soc Remote Sens 40(2):271–285

Argyriou AV, Teeuw RM, Soupios P, Sarris A (2017) Neotectonic control on drainage systems: GIS-based geomorphometric and morphotectonic assessment for Crete, Greece. J Struct Geol 104:93–111

Azor A, Keller EA, Yeats RS (2002) Geomorphic indicators of active fold growth: south Mountain-Oak Ridge Ventura basin, southern California. Geol Soc Am Bull 114:745–753

Bali R, Agrawal KK, Ali SN (2012) Drainage morphometry of Himalayan Glacio-fluvial basin, India: hydrologic and neotectonic implication. Environ Earth Sci 66(4):1163–1174

Balogun IA Adeyewa ZD Balogun AA Morakinyo TE (2011) Analysis of urban expansion and land usechanges in Akure, Nigeria, using remote sensing and GIS technique. J Geograph Reg Plan 4(9):533–541

Bhatt CM, Rajiv C, Sharma PK (2007) Morphotectonic analysis in Anandpur Sahib area, Punjab (India) using remote sensing and GIS approach. Jour Indian Soc Remote Sen 35(2):129–139

Buczek K, Górnik M (2020) Evaluation of tectonic activity using morphometric indices: case study of the Tatra Mts. (Western Carpathians, Poland). Environ Earth Sci 79:1–13

Bull WB (1977) Tectonic geomorphology of the Mojave Desert. U. S. Geological Survey Contract Report 14–08–0001-G-394; Office of Earthquakes, Volcanoes, and Engineering, Menlo Park, California, p.188

Bull WB (1978) Geomorphic tectonic activity classes of the south front of the San Gabriel Mountains, California. U. S. Geological Survey Contract Report 14–08–001- G-394; Office of Earthquakes, Volcanoes, and Engineering, Menlo Park, California, p. 59

Bull WB (2009) Tectonically active landscapes. Wiley-Blackwell, Oxford, p 326

Bull WB, McFadden LM (1977) Tectonic geomorphology north and south of the Oarlock Fault. California J Geomorphology 1:15–32

Burbank DW, Anderson RS (2000) Tectonic geomorphology. Blackwell Scientific, Oxford, p 270

Burbank DW, Anderson RS (2001) Tectonic Geomorphology. Malden: Science 274. (0–632–04386–5)

Canon PJ (1976) Generation of explicit parameters for a quantitative geomorphic study of the Mill Creek drainage basin. Oklahoma Geology Notes 36(1):3–16

Cotton CA (1950) Tectonic scarps and fault valleys. Bull Geol Soc Amer 61:717–758

Cox RT (1994) Analysis of drainage basin asymmetry as a rapid technique to identify areas of possible Quaternary tilt-block tectonics: an example from the Mississippi embayment. Geol Soc Am Bull 106:571–581

Cox RT, Van Arsdale RB, Harris JB (2001) Identification of possible Quaternary deformation in the north eastern Mississippi Embayment using quantitative geomorphic analysis of drainage-basin asymmetry. Geol Soc Am Bull 113(5):615–624

Cuong NQ, Zuchiewicz WA (2001) Morphotectonic properties of the Lo River Fault near Tam Dao in North Vietnam. J Nat Hazards Earth Sys Sci 1:15–22

Das JD, Shujat Y, Saraf AK (2011) Spatial technologies in deriving the morphotectonic characteristics of tectonically active Western Tripura Region, Northeast India. Jour Indian Soc Remote Sen 39:249–258

Dehbozorgi M, Pourkermani M, Arian M, Matkan A, Motamedi H, Hosseiniasl A (2010) Quantitative analysis of relative tectonic activity in the Sarvestan area, central Zagros Iran. Geomorphology 121:329–341

Demoulin A (2011) Basin and river profile morphometry: a new index with a high potential for relative dating of tectonic uplift. Geomorphology 126:97–107

Duncan C, Masek J, Fielding E (2003) How steep are the Himalaya? Characteristics and of along-strike topographic variations. Geology 31:75–78

El-Hamdouni R, Irigaray C, Fernández T, Chacón J, Keller EA (2008) Assessment of relative active tectonics, southwest border of the Sierra Nevada (southern Spain). Geomorphology 96:150–173

Faghih A, Soudejani AE, Nourbakhsh A, Rokni S (2015) Tectonic geomorphology of High Zagros Ranges, SW Iran: an Initiative towards Seismic Hazard Assessment. Environ Earth Sci 74:3007–3017

Ganas A, Pavlides S, Karastathis V (2005) DEM-based morphometry of range-front escarpments in Attica, central Greece, and its relation to fault slip rates. Geomorphology 65:301–319

Gayen S, Bhunia GS, Shi PK (2013) Morphometric analysis of Kangshabati-Darkeswar interfluves area in West Bengal, India using ASTER DEM and GIS techniques. Geol Geosci 2(4):1–10

Geurts AH, Cowie PA, Duclaux G, Gawthorpe RL, Huismans RS, Pedersen VK, Wedmore LNJ (2018) Drainage integration and sediment dispersal in active continental rifts: a numerical modelling study of the central Italian Apennines. Basin Res 30(5):965–989

GSI (2002) District Resource map of Chandrapur, District Geological Survey of India, Publication

Hare PW, Gardner TW (1985) Geomorphic indicator of vertical neotectonism along converging plate margins, Nicoya Peninsula, Costa Rica. Pp. 75–104. In Tectonic Geomorphology: Proceedings of the 15th Annual Binghamton Geomorphology Symposium, volume 15

Hooper DM, Bursik MI, Webb FH (2003) Application of high resolution interferometric DEMs to geomorphic studies of fault scarps,

Fish Lake Valley, Nevada-California, USA. Remote Sens Environ 84:255–267
Jackson JA, Leeder M (1993) Drainage systems and the development of normal faults: An example from Pleasant valley, Nevada. J Struct Geol 16:1041–1059
Jain V, Sinha R (2005) Evaluation of geomorphic control on flood hazard through geomorphic instantaneous unit hydrograph. Current Sci 85(11):26–32
Kale VS, Sengupta S, Achyuthan H, Jaiswal MK (2014) Tectonic controls upon Kaveri River drainage, cratonic Peninsular India: Inferences from longitudinal profiles, morphotectonic indices, hanging valleys and fluvial records. Geomorphology 227:153–165
Keller E (1986) Investigation of active tectonics: use of surfacial earth processes. In: Re W (ed) Active tectonics studies in Geophysics. National Academy Press, Washington, D.C., pp 136–147
Keller EA, Pinter N (1996) Active tectonics: earthquakes uplift and landscapes. Prentice Hall, New Jersey
Keller EA Pinter N (2002) Active tectonics: earthquakes, uplift, and landscape. Prentice Hall, New Jersey. p. 362
Kumar B, Venkatesh M, Triphati A, Anshumali, (2017) A GIS-based approach in drainage morphometric analysis of Rihand River Basin. Central India Sustain Water Resour Manag 4(1):45–54
Litchfield NJ, Campbell JK, Nicol A (2003) Recognition of active reverse faults and folds in North Canterbury, New Zealand, using structural mapping and geomorphic analysis. New Zeal J Geol Geophys 46(4):563–579
Liu Y, De Smedt F (2005) Flood modeling for complex terrain using GIS and remote sensed information. Water Resour Manag 19:605–624
Magesh NS, Chandrasekar N (2014) GIS model based morphometric evaluation of Tamiraparani subbasin, Tirunelveli district, Tamil Nadu, India. Arab J Geosci 7:131–141
Mahala A (2020) The significance of morphometric analysis to understand the hydrological and morphological characteristics in two different morpho-climatic settings. Appl Water Sci 10:33
Manjare BS (2013) Mapping of Lineaments in some part of Betul District, Madhya Pradesh and Amravati District of Maharashtra, Central India, using remote sensing and GIS techniques. Int J Adv Remote Sens GIS 2(1):331–340
Manjare BS (2014) Tectonic Geomorphology in North East Part of Salbardi Fault Central India Using Remote Sensing and GIS Approach. Jour Ind Geol Cong 6(1):47–55
Manjare BS (2015) Morphotectonic analysis of upper Tapi River subbasin, Madhya Pradesh. Central India J Geosci Res 1(1):81–88
Manjare BS (2017) Drainage Characteristics of Tectonically Active Areas in Wardha and Purna River Basin, Central India Using of Satellite Data. J Geomat 11(2):260–267
Matoš B, Tomljenović B, Pérez-Peña JV (2016) Landscape response to recent tectonic deformation in the SW Pannonian Basin: evidence from DEM based morphometric analysis of Bilogora Mt. area, NE Croatia. Geomorphology 263:132–155
Menéndez I, Silva PG, Martín-Betancor M, Pérez-Torrado FJ, Guillou H, Scaillet S (2008) Fluvial dissection, isostatic uplift, and geomorphological evolution of volcanic islands (Gran Canaria, Canary Islands, Spain). Geomorphology 102:189–203
Molin P, Fubelli G (2005) Morphometric evidence of the topographic growth of the Central Apennines. Geogr Fis Din Quat 28:47–61
Muller JE (1968) An introduction to the hydraulic and topographic sinuosity indexes. Annals Assoc Am Geog 58:371–385
Pande, C, Kanak M, Pande R. (2018) Assessment of morphometric and hypsometric study for watershed development using spatial technology-a case study of Wardha River basin in Maharashtra, India. Int J River Basin Manage, 1–11
Perez-Pena JV, Azor A, Azanon JM, Keller EA (2010) Active tectonics in the Sierra Nevada (Betic Cordillera, SE Spain): Insights from geomorphic indexes and drainage pattern analysis. Geomorphology 119:74–87
Prakash K, Mohanty T, Singh S, Chaubey K, Prakash P (2016) Drainage morphometry of the Dhasan River basin, Bundelkhand craton, central India using remote sensing and GIS techniques. J Geomat 10:21–132
Raj R, Bhandari S, Maurya DM, Chamyal LS (2003) Geomorphic indicators of active tectonics in the Karjan River Basin, Lower Narmada Valley, western India. J Geol Soc India 62:739–752
Ramírez-Herrera MT (1998) Geomorphic assessment of active tectonics in the Acambay graben, Mexican Volcanic Belt. Earth Surf Proc Land 23:317–332
Reddy GPO (2018) Remote sensing and GIS in digital terrain modeling, In: Reddy G.P.O. and Singh S.K. (Eds.) Geospatial technologies in land resources mapping, monitoring and management. Geotechnologies and the environment, Vol 21. Springer, Cham, pp. 201–222
Reddy GPO, Maji AK (2003) Delineation and characterization of geomorphological features in a part of lower Maharashtra metamorphic plateau, using IRS-ID LISS-III data. Jour Indian Soc Remote Sen 31(4):241–250
Reddy GPO, Maji AK, Gajbhiye KS (2002) GIS for morhophometric analysis of river basins. GIS India 11(9):9–14
Reddy GPO, Maji AK, Gajbhiye KS (2004) Drainage morphometry and its influence on landform characteristics in Basaltic Terrain – A Remote Sensing and GIS Approach. Int J Appl Earth Obs Geoinf 6:1–16
Reddy GPO, Kumar N, Sahu N, Singh SK (2018) Evaluation of automatic drainage extraction thresholds using ASTER GDEM and Cartosat-1 DEM: A case study from basaltic terrain of Central India. Egypt J Remote Sen Space Sci 21(1):95–104
Repasch M, Karlstrom K, Heizler M, Pecha M (2017) Birth and evolution of the Rio Grande fluvial system in the past 8 Ma: progressive downward integration and the influence of tectonics, volcanism, and climate. EarthSci Rev 168:113–164
Rockwell T, Keller E, Jhonson D (1984) Tectonic geomorphology of alluvial fans and mountain fronts near Ventura, California. (Eds. Morisawa, M. and Hack. T.J.), Tectonic Geomorphology. Publ. in Geomorphology, State Union of New York, Binghamton, pp. 183–207
Roy S, Sahu AS (2015) Quaternary tectonic control on channel morphology over sedimentary low land: a case study in the Ajay-Damodar interfluve of Eastern India. Geosci Front 6(6):927–946
Schumm SA, Dumont JF, Holbrook JM (2000) Active tectonics and alluvial rivers. Cambridge University Press, Cambridge, p 276
Scotti VN, Molin P, Faccenna C, Soligo M, Casas-Sainz A (2014) The influence of surface and tectonic processes on landscape evolution of the Iberian Chain (Spain): quantitative geomorphological analysis and geochronology. Geomorphology 206:37–57
Sharma S, Sarma JN (2017) Application of Drainage Basin Morphotectonic Analysis for Assessment of Tectonic Activities over Two Regional Structures of the Northeast India. Jour Geol Soc India 89:271–280
Shradha MK (2019) Tectonic geomorphology in some part of Warhdha River, Central India, Using GIS and Remote sensing techniques Unpublished Dissertation Thesis submitted to RTM Nagpur University, Nagpur P., 39
Siddiqui S (2014) Appraisal of active deformation using DEM-based morphometric indices analysis in Emilia-Romagna Apennines, Northern Italy. Geodyn Res Int Bull1(3), XXXIVeXLII
Silva PG, Goy JL, Zazo C, Bardaji T (1992) Fault-generated mountain fronts in southeast Spain: geomorphologic assessment of tectonic and seismic activity. Geomorphology 50:203–225
Singh B, Dowerah J (2010) ASTER DEM based studies for geological investigation around Singhbhum Shear Zone (SSZ) in Jharkhand. India J Geogr Inf Sys 2(1):11–14

Suganthi S, Srinivasan K (2010) Digital elevation model generation and its application in landslide studies using Cartosat-1. Int J Geomatics and Geosci 1(1):41–50

Susan R (1993) Geomorphic observations of rivers in the Oregon coast range from a regional reconnaissance perspective. Geomorphology 6:135–150

Tepe C, Sozbilir H (2017) Tectonic geomorphology of the Kemalpaşa Basin and surrounding horsts, southwestern part of the Gediz Graben, Western Anatolia, Informa UK Limited, trading as Taylor & Francis Group; 29(1): 70–90

Wallace RE (1978) Geometry and rates of change of fault-related fronts, north-central Nevada. J Res US Geol Surv 6:637–650

Wells SG, Bullard TF, Menges CM, Drake PG, Karas PA, Kelson KI (1988) Regional variations in the tectonic geomorphology along a segmented convergent plate boundary, Pacific Coast of Costa Rica. Geomorphology 1:239–265

Youssef AM, Pradhan B, Sefry SA (2016) Flash flood susceptibility assessment in Jeddah city (Kingdom of Saudi Arabia) using bivariate and multivariate statistical models. Environ Earth Sci 75:12